Corrosion of Commercial Stainless Steel AISI 310 and of a V-Modified Fe-Ni-Cr Model Alloy in Coal Gasification Type Atmospheres at 600°C

L.C. Li[1,2], F. Gesmundo[1,4], F. Viani[1] and G.P. Toledo[3]

[1]*Institute of Chemistry, Faculty of Engineering, University of Genova, Fiera del Mare, Pad. D, 16129 Genova, Italy*
[2]*Department of Surface Science and Corrosion Engineering, The University of Science and Technology Beijing, 30 Xue Yuan Lu, 100083 Beijing, China*
[3]*ENEL-CRTN, Via Rubattino 24, 20134 Milan, Italy*

ABSTRACT

Corrosion of commercial stainless steel 310 SS and of a model alloy based on iron and nickel but containing also a large concentration of chromium plus some vanadium was studied at 600°C in two mixed sulfidizing-oxidizing gases simulating the composition of the atmospheres typical of coal gasification and containing 0.4 and 1 vol. % H_2S, respectively. In both cases, the alloys underwent a sulfidation attack with very little or no oxidation. Moreover, the corrosion rates of the two alloys in these environments were very similar. However, the vanadium-containing alloy, which was also richer in nickel and lower in iron than 310 SS, formed a thick, very porous outer layer in addition to an inner compact region similar to that observed for 310 SS. Thus, we concluded that the presence of vanadium is practically ineffective, while that of nickel, which seems to be responsible for the growth of the outer porous layer, is detrimental under sulfidizing conditions.

Key Words: corrosion, coal gasification, stainless steel

1. INTRODUCTION

The atmospheres prevailing in coal gasification plants and especially in gas cooler sections are particularly aggressive towards most common materials for high temperature applications due to their tendency to produce sulfidation rather than oxidation /1-6/. In fact, the formation of sulfides either alone or in mixture with oxides is generally associated with very fast corrosion rates /1-6/ as a consequence of the large deviations from stoichiometry and of the large diffusion rates presented by most transition metal sulfides /7,8/. The results of earlier corrosion studies carried out at 800°C and above led to the conclusion that no material could withstand these environments of high sulfur partial pressures coupled to very low oxygen pressures /1-6,9/. More recently, attention was directed towards much lower temperatures where some materials were sufficiently resistant to survive the long lifetimes planned for industrial plants /9-11/. Stainless steel 310 as well as alloy 800 are among the materials so far most frequently studied in view of their good high-temperature properties, including also their good corrosion resistance to oxidizing environments due to their rather high chromium content. However, even these materials may undergo very fast corrosion if the gas composition is not favorable, i.e., if the partial pressure of sulfur is too high as compared to the oxygen partial pressure /1-6,12/. Thus, a search for other, more sulfidation-resistant materials is still being conducted for this particularly demanding application. Recently, it was suggested that the addition of relatively low concentrations of refractory

[4]To whom all correspondence should be addressed

elements to high-chromium alloys may significantly improve their resistance to corrosion in coal gasification atmospheres /13-15/. The present paper presents the results of a study on corrosion in two simulated coal-gasification environments of the commercial steel 310 SS and of a new model alloy based on iron and nickel and rather high in chromium containing a significant addition of vanadium in order to assess the effects of the presence of vanadium on the corrosion behavior of two high-temperature materials of rather similar composition.

2. EXPERIMENTAL

The alloys tested included the commercial stainless steel AISI 310 (310 SS) and a model Fe-Ni-Cr alloy containing also vanadium prepared by Sumitomo Heavy Industries (Japan) in collaboration with EPRI (USA), which was kindly donated by W.T. Bakker of EPRI. The composition of the two alloys is shown in Table 1. Samples were 20x10x1 mm in size and were machined from larger pieces. Before each test they were ground down to 600 grit paper, cleaned in alcohol and dried. Corrosion tests were carried out both in a Cahn thermobalance mod. 2000 with continuous weight-gain measurements and in a horizontal furnace with discontinuous measurements at non-uniform intervals for times up to 250 h. For each corrosion test, new samples were used to avoid complications due to partial scale spalling during cooling at the end of each experiment.

The corrosion atmospheres were composed of H_2-CO_2-H_2S mixtures of appropriate composition. Two different gases were used, containing respectively 92.6 vol.% H_2, 7% CO_2 and 0.4% H_2S (mixture 1) and 92% H_2, 7% CO_2 and 1% H_2S (mixture 2). Under conditions of equilibrium at 600°C, they produced oxygen and sulfur pressures equal to 4.1x10-26 and 7.2x10-11 atm (mixture 1) and 4.1x10-26 and 4.6x10-10 atm (mixture 2), respectively. For the thermobalance tests, the reaction chamber (quartz tube) was first evacuated, while the sample was kept at room temperature and the furnace brought separately to the reaction temperature. After this, the reaction chamber was first filled with pure nitrogen from the top of the balance and then the corrosion mixture was introduced from the bottom of the tube. The two gases were mixing well above the sample level before leaving the quartz tube. After about 30 min of gas flow, the furnace was raised to the sample level and the reaction started. The procedure adopted for the tests in the horizontal furnace was different, due to the long time required by the furnace to warm up to the test temperature (about 2.5 h). Initially, after introducing the samples, the tube was evacuated and kept under vacuum until the furnace reached the corrosion temperature, after which it was filled with the corrosion mixture. However, for 310 SS this procedure did not produce results in good agreement with those obtained by means of the thermobalance. A possible reason for this was that the samples could undergo an initial oxidation. Thus a different procedure was adopted, which consisted of warming up the sample directly in the corroding gas mixture to avoid a possible purely oxidizing initial stage. This procedure gave more meaningful results and was finally used for all tests in the horizontal furnaces.

The corroded samples were then examined by means of X-ray diffraction and were then mounted in epoxy resins, sectioned and polished metallographically for examination under the optical and scanning electron microscopes and by means of an EDX attachment to the SEM.

Table 1

Composition of the alloys used in the present study (Fe balance)

	Cr	Ni	Mn	Si	C	V	Nb
310 SS	23.34	18.15	.69	1.67	.063	-	-
Model alloy	26	39	.60	.27	.05	3.1	.22

3. RESULTS

1. Corrosion kinetics

The kinetic curves for corrosion in the thermobalance of the two alloys in the two atmospheres used

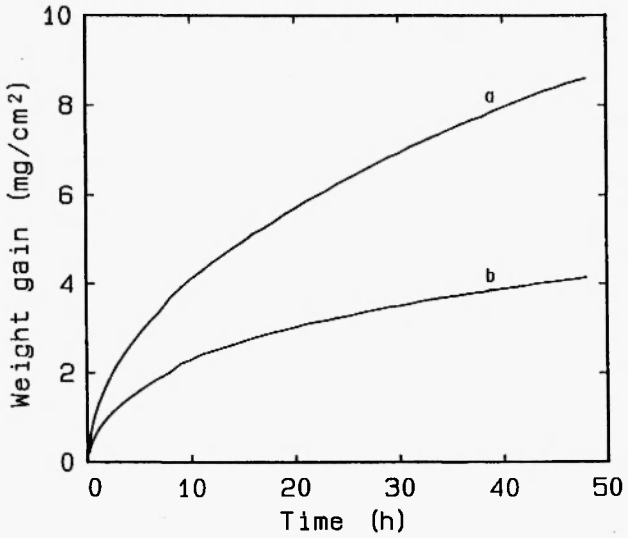

Fig. 1: Kinetic curves for stainless steel 310 SS (curve a) and the V-modified Fe-Ni-Cr alloy (curve b) corroded for 48 h in the thermobalance in the gas mixture 1 at 600°C.

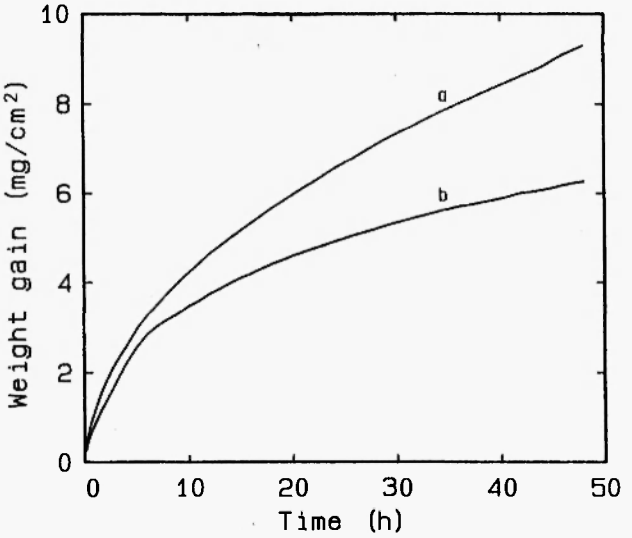

Fig. 2: Kinetic curves for stainless steel 310 SS (curve a) and the V-modified Fe-Ni-Cr alloy (curve b) corroded for 48 h in the thermobalance in the gas mixture 2 at 600°C.

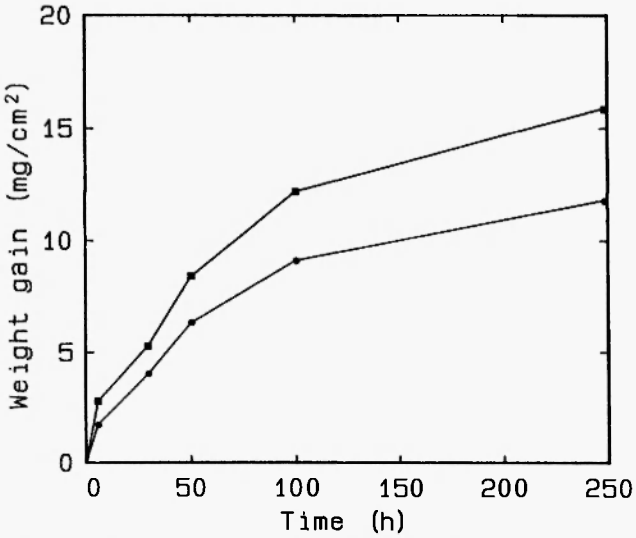

Fig. 3: Kinetic curves for stainless steel 310 SS and the V-modified Fe-Ni-Cr alloy corroded for 250 h in a horizontal furnace in the gas mixture 1 at 600°C. ■: 310 stainless steel; ●: V-modified Fe-Ni-Cr alloy.

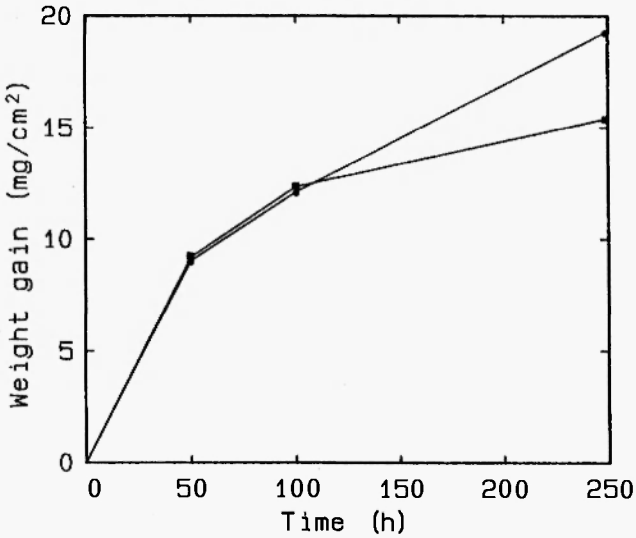

Fig. 4: Kinetic curves for stainless steel 310 SS and the V-modified Fe-Ni-Cr alloy corroded for 48 h in a horizontal furnace in the gas mixture 1 at 600°C. ■: 310 stainless steel; ●: V-modified Fe-Ni-Cr alloy.

in the present work for reaction times up to 48 h are shown in Figs. 1 and 2.Corrosion of a 310 SS followed a good parabolic rate low in both gas mixtures, with parabolic rate constants equal to 4.4×10^{-10} and 5.0×10^{-10} $g^2cm^{-4}s^{-1}$ for mixtures 1 and 2, respectively. The V-modified model alloy corroded more slowly than 310 SS but showed significant deviations from a parabolic rate law with average rate constants equal to 7.8×10^{-11} and 1.5×10^{-10} $g^2cm^{-4}s^{-1}$, respectively.

The kinetic results for corrosion in the horizontal furnace for times up to 250 h are shown in Figs. 3 and 4 for the two mixtures. The corrosion of 310 SS did not

follow a good parabolic rate law, because the instantaneous rate constant decreased with time. The average rate constants calculated for the whole corrosion period for this material are equal to 2.9×10^{-10} and 2.5×10^{-10} $g^2cm^{-4}s^{-1}$ for mixtures 1 and 2, respectively. Corrosion of the V-modified model alloy in mixture 1 showed essentially two parabolic stages with rate constants equal to 2.3×10^{-10}(first stage) and 1.1×10^{-10} $g^2cm^{-4}s^{-1}$ (second stage). Corrosion in mixture 2 followed a single parabolic stage with a rate constant equal to 4.3×10^{-10} $g^2cm^{-4}s^{-1}$. Altogether the model alloy corroded more slowly than 310 SS in the thermobalance tests in both gas mixtures and in the furnace tests with the mixture containing 0.4 vol.% H_2S. In the furnace tests with the 1 vol.% H_2S mixture, the two steels had approximately the same rate up to 100 h, but after 250 h the model alloy had a weight gain higher than 310 SS. Finally, for both materials the corrosion rates increased with the H_2S content of the gas and were quite high, with weight gains of the order of 15-20 mg/cm^2 after 250 h corrosion.

2. *Scale structure and composition*

The structure of the scales formed on 310 SS after 50 h corrosion in the horizontal furnace in mixture 1 and the corresponding X-ray maps of the element distribution are shown in Fig. 5. The scale presents two main layers plus a region of internal attack in the alloy. The combination of the results of X-ray diffraction and microprobe analysis permits us to conclude that the outer layer is composed of FeS containing some Cr in solution (5-8 at % Cr), while the inner layer is made of Fe-Cr thiospinel with a composition corresponding to the nearly stoichiometric $FeCr_2S_4$. The alloy surface presents a strong enrichment in nickel and silicon and is depleted in Fe. The precipitated particles are of Cr sulfide which may possibly contain some iron. Nickel is essentially confined to the alloy surface region, but some nickel (up to 15 at %) exists also in the scales, especially along the grain boundaries and/or the lines of fracture in the outer sulfide layer. The same scale structure is observed even after longer corrosion times in the same mixture.

The scales formed on 310 SS after 48 h corrosion

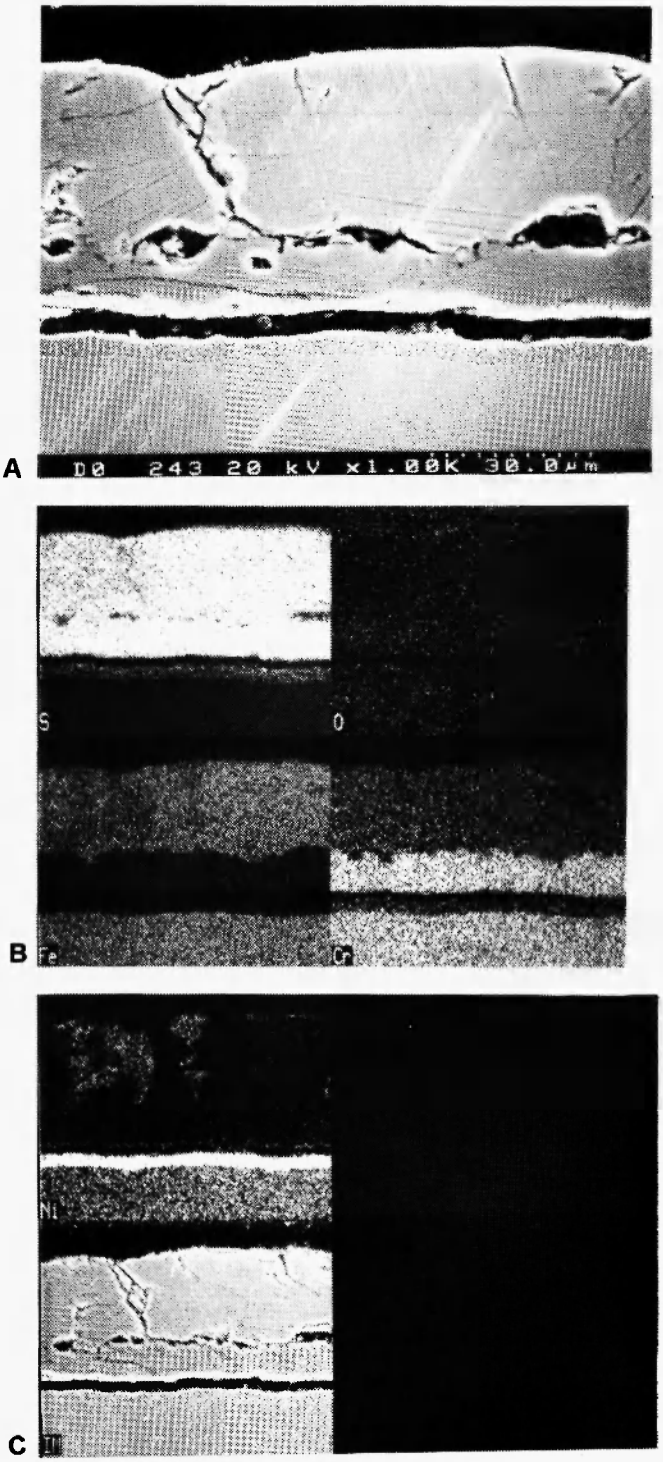

Fig. 5: Cross-section of 310 stainless steel after 50 h corrosion in a horizontal furnace in the gas mixture 1. a: SEM micrograph; b: X-ray maps of S, O, Fe and Cr; c: SEM image and X-ray map of Ni.

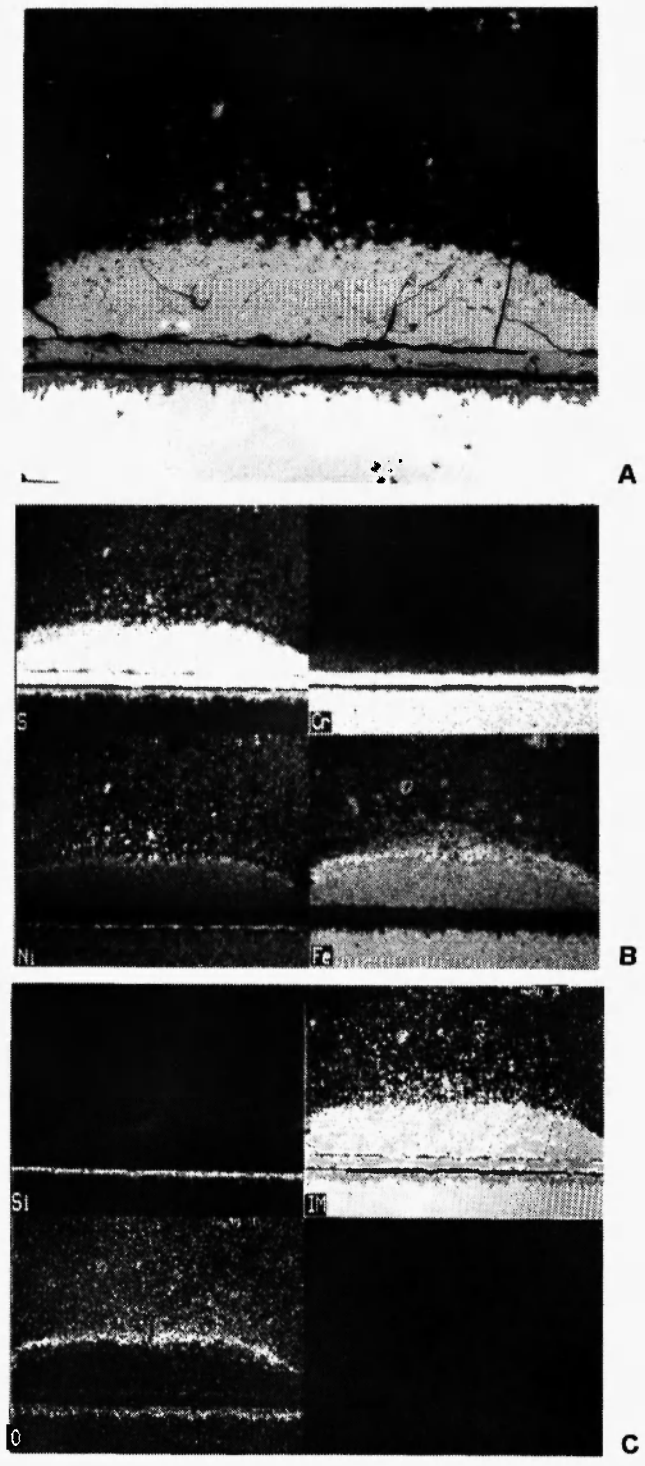

Fig. 6: Cross-section of 310 stainless steel after 100 h corrosion in a horizontal furnace in the gas mixture 2. a: BEI image; b: X-ray maps of S, Cr, Ni and Fe; c: SEM image and X-ray maps of Si and O.

in mixture 2 are similar to those grown after exposure to mixture 1 examined previously. However, after longer corrosion times a different structure is observed on some regions of the sample surface, as shown in Fig. 6 for a sample reacted for 100 h. In these points, the scale is thicker than usual and presents an outer porous region containing a mixed sulfide of iron and nickel. The distribution of iron and chromium in the inner scale zone is similar to that observed in the more dilute mixture, but the innermost scale layer contains more chromium than previously, while the zone of internal attack also contains some oxide in addition to chromium sulfide. Finally, the outer surface of the compact scale also contains some oxygen associated with iron. An enlarged view of the same nodule (Fig. 7) shows more clearly the distribution of the elements in the inner compact scale zone and in particular the presence of a significant concentration of nickel (10-11 at %) at the outer surface of the compact scale region.

The scales grown on the V-modified model alloy after 50 h corrosion in the horizontal furnace in mixture 1 are shown in Fig. 8; the inner compact zone is shown in more detail in Fig. 9. The outermost layer is very thick, quite porous and contains a mixed sulfide of iron and nickel. The outer zone of the inner compact scale contains more nickel than in the previous material (up to 26-27 at %), while the inner region is composed of a mixture of the iron-chromium thiospinel and of chromium sulfide containing 45-47 at % Cr and 6-7 at % V and 4-5 at % Fe. Chromium sulfide, but not chromium oxide precipitates, are again present in the surface layer of the alloy where nickel is still enriched. Vanadium is distributed only in the Cr-rich inner layer of the compact scale zone. After 50 h corrosion in mixture 2, the scale presents again a thick porous outer zone of iron and nickel sulfides and an inner compact region (Fig. 10). The latter contains an outer irregular layer of iron and nickel sulfides and an internal region of iron-chromium thiospinel. The innermost layer in contact with the alloy is made of chromium sulfide with vanadium in solution. Traces of iron oxides are also observed at the outer surface of the compact layer. After 100 h corrosion (Fig. 11), the general scale structure is similar. An enlarged view of the inner layer (Fig. 12) shows an outer region of FeS

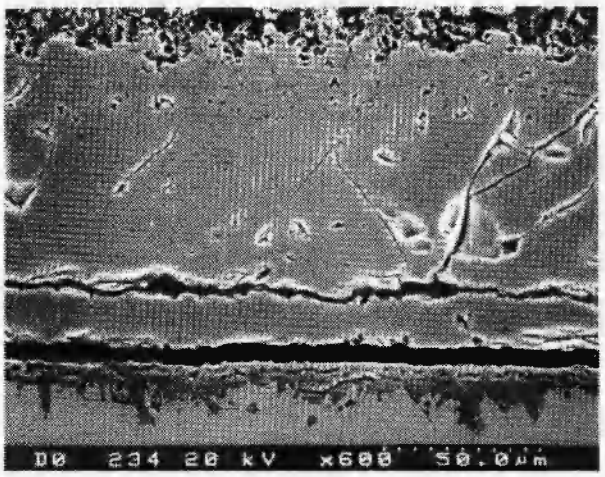

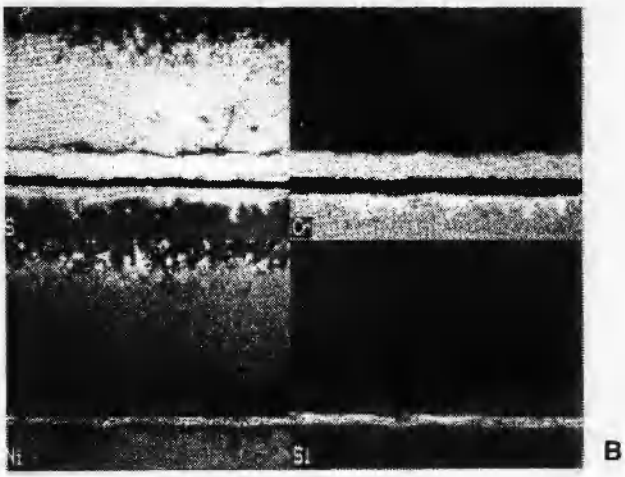

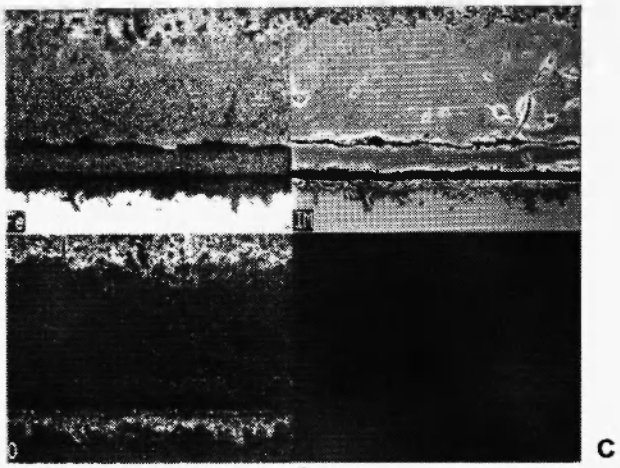

Fig. 7: Enlarged view of the nodular region shown in Fig. 6. a: SEM image; b: X-ray maps of S, Cr, Ni and Si; c: SEM image and X-ray maps of Fe and O.

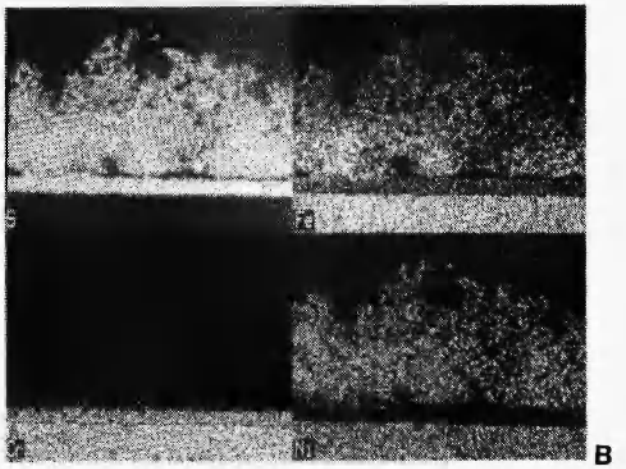

Fig. 8: Cross-section of V-modified Fe-Ni-Cr alloy after 50 h corrosion in a horizontal furnace in the gas mixture 1. a: SEM image; b: X-ray maps of S, Fe, Cr and Ni.

containing nickel (8 at %) and Cr (8 at %), an intermediate layer of Fe-Cr thiospinel followed by another layer of chromium sulfide (20 at % Cr) with a high content of vanadium (13-14 at %) and a relatively low content of both Fe and Ni (about 5-8 at % each). Finally, the innermost layer is of chromium sulfide (41 at % Cr) with vanadium (6-7 at %) and iron (4-5 at %) in solution. Oxygen is again present both in the innermost region associated with chromium and in the external region associated with iron.

4. DISCUSSION

Corrosion in 310 SS of H_2-H_2S mixtures has

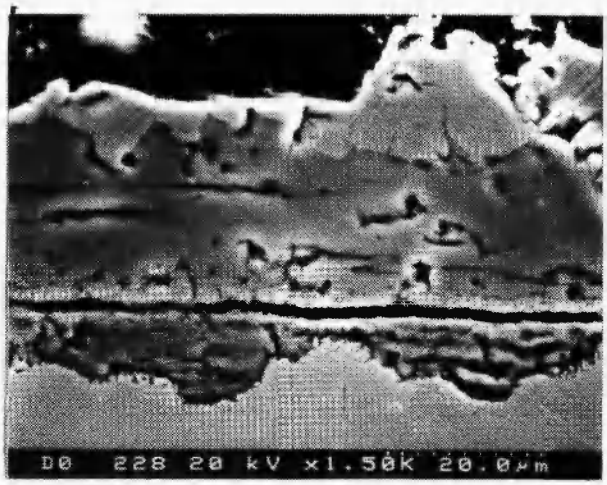

A

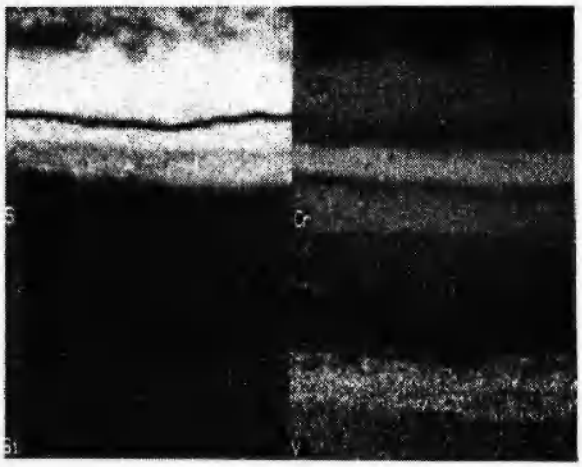

B

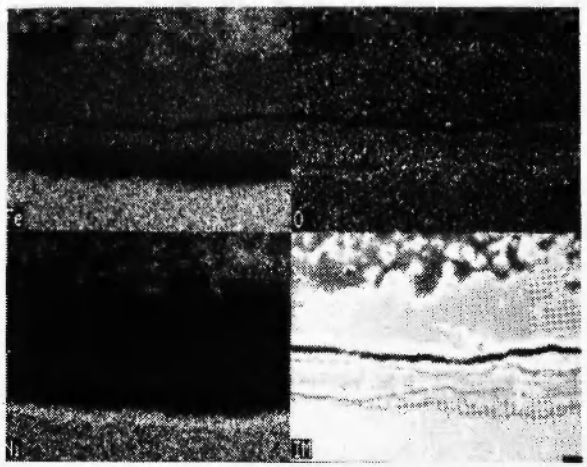

C

Fig. 9: Enlarged view of Fig. 8. a: SEM image; b: X-ray maps of S, Cr, Si and V; c: SEM image and X-ray maps of Fe, O and Ni.

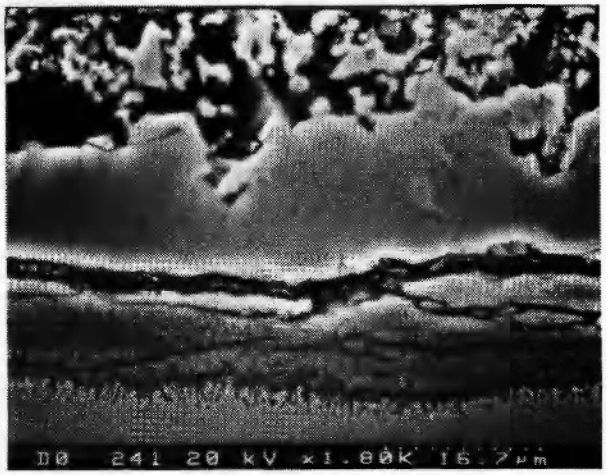

A

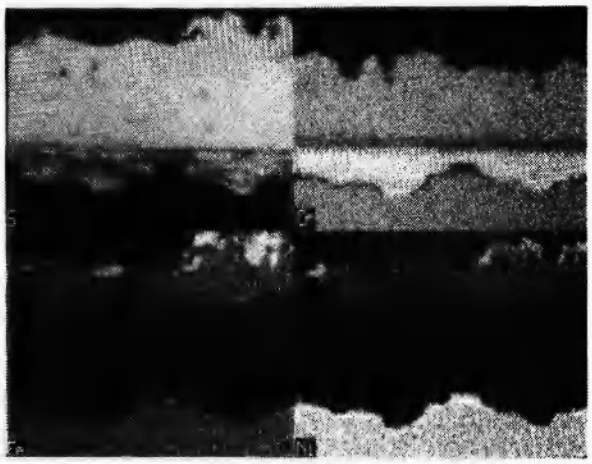

B

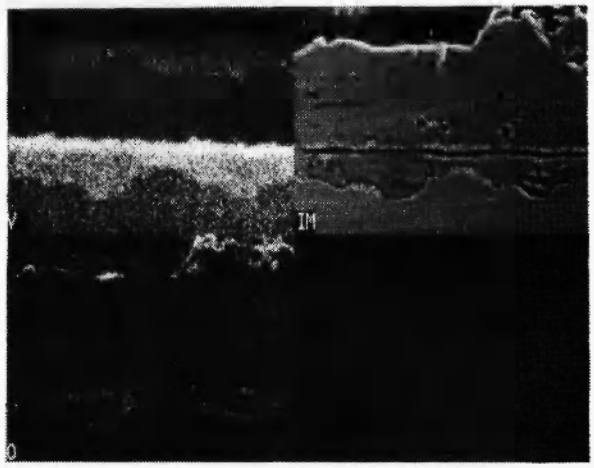

C

Fig. 10: Cross-section of V-modified Fe-Ni-Cr alloy after 50 h corrosion in a horizontal furnace in the gas mixture 2. a: SEM image; b: X-ray maps of S, Cr, Fe and Ni; c: SEM image and X-ray maps of V and O.

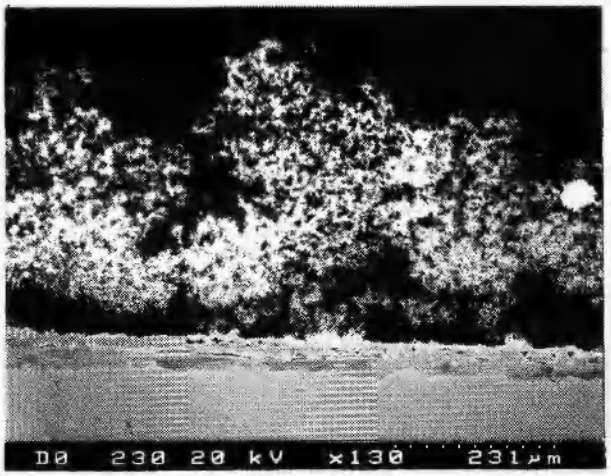

A

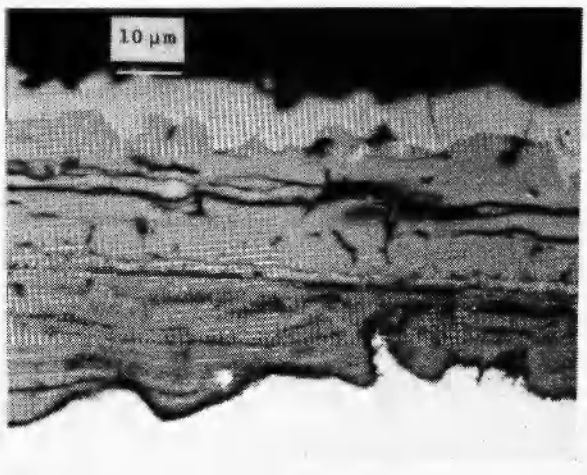

A

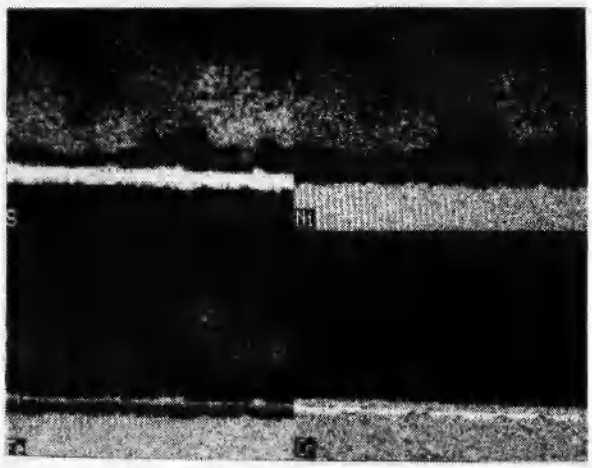

B

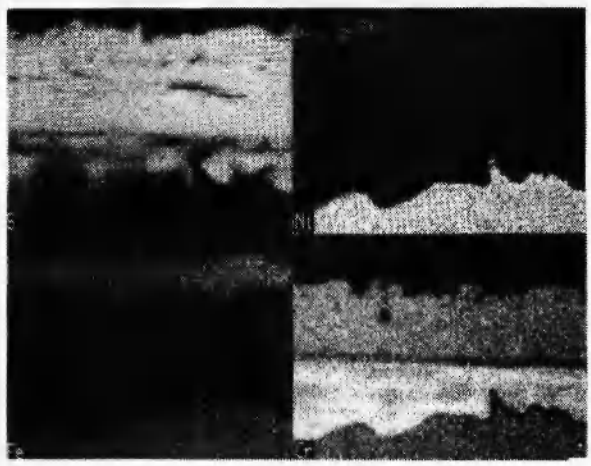

B

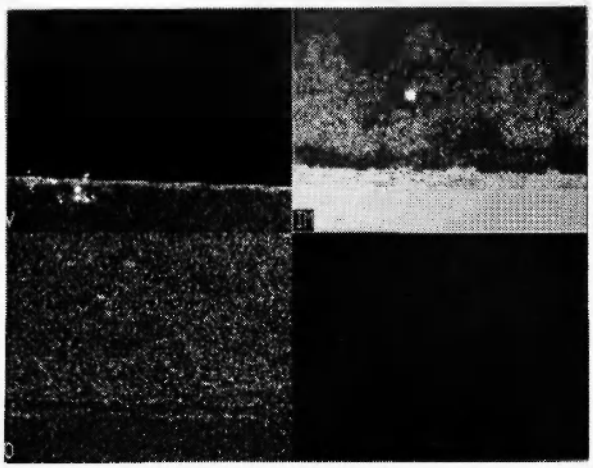

C

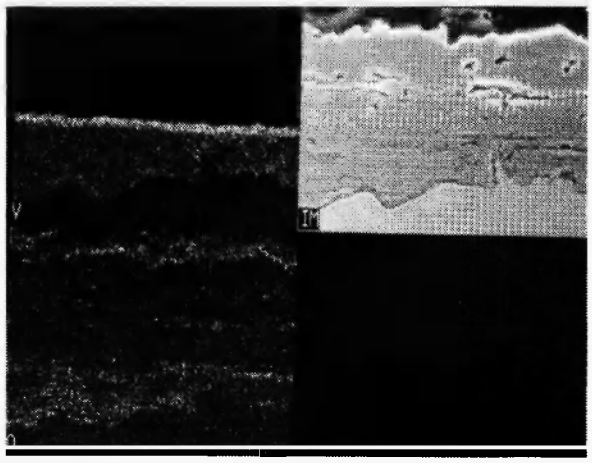

C

Fig. 11: Cross-section of V-modified Fe-Ni-Cr alloy after 100 h corrosion in a horizontal furnace in the gas mixture 2. a: SEM image; b: X-ray maps of S, Ni, Fe and Cr; c: SEM image and X-ray maps of V and O.

Fig. 12: Enlarged view of Fig. 11. a: BEI image; b: X-ray maps of S, Ni, Fe and Cr; c: SEM image and X-ray maps of V and O.

already been studied between 612 and 1012°C under different sulfur pressures by Rao and Nelson /16,17/; their results were summarized briefly by Young in a review paper on the sulfidation behavior of iron and its alloys /18/. The sulfidation of this steel follows a parabolic rate law after an initial stage during which the instantaneous rate constant increases with the reaction time /17/. The structure of the scales depends on both the corrosion temperature and the sulfur pressure in the gas; in general, they contain one or two external layers plus a zone of internal attack /17,18/. The outermost layer forms only below 872°C and under sulfur pressures above 10^{-7} atm. Below 792°C the outer scale layer consists of a mixture of (Fe,Ni)S and $(Fe,Ni)_9S_8$ (pentlandite), while above 792°C only pentlandite forms, which, however, melts above 872°C /17,18/. The inner layer is composed of iron-chromium thiospinel $Fe_{1+x}Cr_{2-x}S_4$ mixed with the chromium sulfide Cr_2S_3, but under some conditions it also contains particles of metallic iron and nickel, which form during cooling /17,18/. In any case, 310 SS has the highest resistance to high-temperature sulfidation among the stainless steels /18/.

Corrosion of this steel in mixed oxidizing-sulfidizing environments typical of coal gasification has been studied extensively with reference to its possible use in the construction of coal gasification plants and notably of the gas-cooler section /6,12/. The results available in the literature up to 1989 were collected and critically analyzed by Gesmundo in a report written for the European Community /12/ and presented in a shorter form more recently /6/. As for other materials which contain sufficient chromium to form outer chromia scales in oxidizing environments, the behavior of 310 SS in coal gasification atmospheres depends critically on the corrosion temperature and on the gas-phase composition. In fact, this form of corrosion may lead either to the formation of essentially oxide scales mainly composed of chromia or of scales containing a mixture of oxides and sulfides or even sulfides only. These modifications of the scale structure are associated with quite large changes in the metal corrosion rate because the simple oxidation is quite protective, while the formation of mixed or of purely sulfide scales corresponds generally to quite high metal consumption rates /1-6,9-15/.

As a result of many experimental studies, the conditions for the growth of protective Cr_2O_3 scales for chromia-forming alloys exposed to coal-gasification environments have been established /1-6, 9-15/. The gas composition required for this must not only fall within the field of stability of chromium oxide in the isothermal phase stability diagram of the relevant M-O-S system, but must also lie sufficiently far from the line corresponding to the thermodynamic equilibrium between the oxide and the sulfides of chromium /1-6,9-15,19/. The line which in the phase diagram divides the region of gas compositions corresponding to the formation of oxide scales from those where sulfide or sulfide-oxide mixed scales form is known as the kinetic boundary /1-6,9-15,19/. For chromia-formers the kinetic boundary is approximately parallel to the chromium oxide-chromium sulfide equilibrium line, but its location is a function of temperature and of the alloy composition /1-6,9-15,19/. In particular, the location of the kinetic boundary for 310 SS has already been established at some temperatures /6,12,20-22/. The superimposed phase diagram for the Cr-O-S, Fe-O-S and Ni-O-S systems at 600°C is shown in Fig. 13. The oxygen

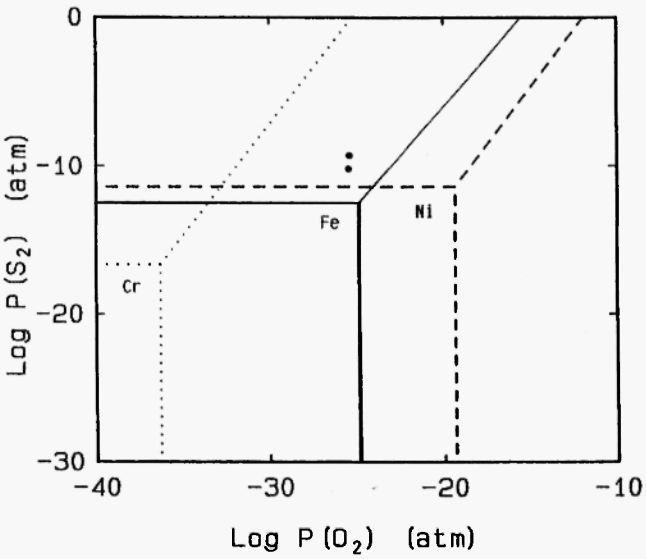

Fig. 13: Superimposed isothermal phase diagrams of the Cr-O-S (dotted lines), Fe-O-S (solid lines) and Ni-O-S (dashed lines) systems at 600°C with an indication of the composition of the gas mixtures used.

pressure produced by the present gas mixtures is in the field of stability of Cr_2O_3 but below the stability of both the iron and nickel oxides, while the sulfur pressure is above the dissociation pressure of all sulfides. According to the phase diagram, the phases stable in both gases are the oxide of chromium and the sulfides of both iron and nickel.

Corrosion of 310 SS in coal gasification atmospheres with H_2S contents ranging between 0.2 and 2 vol % was examined recently /23-25/. The partial pressure of O_2 used in these works was $1.7x10^{-26}$ atm, while that of sulfur was equal to 10^{-11}, $7x10^{-11}$, $1.5x10^{-10}$, $4x10^{-10}$ and $1x10^{-9}$ atm for initial H_2S additions of 0.2, 0.4, 0.6, 1 and 2 vol %, respectively, to a base mixture containing 7 vol % CO, 1.5 vol % H_2O and balance H_2 /23-25/. These measurements showed that the corrosion of this material in mixtures containing 0.4 vol % H_2S leads to the formation of oxide scales containing mainly Cr_2O_3 at low corrosion rates, with an approximate parabolic rate constant equal to $7x10^{-14}$ $g^2cm^{-4}s^{-1}$ /25/. Only after 100 h, the surface of the scale started to present sulfide nodules rich in chromium, which became larger and more numerous as the reaction time increased /25/. On the contrary, corrosion in mixtures containing 1 vol % H_2S led to the formation of scales composed of sulfides of iron and chromium with small nickel contents and of internal oxide and sulfide of chromium and in some cases of a thin and discontinuous layer of chromium oxide /25/. The corrosion kinetics were parabolic with a rate constant equal to 10^{-10} $g^2cm^{-4}s^{-1}$ /25/.

The results of the present study are in substantial agreement with those of previous works /23-25/ regarding corrosion in the mixture containing 1 vol % H_2S, but not for the more dilute mixture, because the scales formed in mixture 1 used in the present investigation again contained mostly sulfides, while the corrosion rate was much higher than that corresponding to the growth of chromia scales. The reasons for this difference are not clear. In fact, the oxygen pressure prevailing in the present mixture containing 0.4 vol % H_2S ($4.1x10^{-26}$ atm) is slightly higher than that used in previous measurements ($1.7x10^{-26}$ atm), while the sulfur pressures are practically the same; therefore, the present gas composition is even more favorable to oxidation. The simplest assumption is that the gas mixtures do not equilibrate completely at the reaction temperature, as already proposed in view of the low rate of some reactions in the gas phase /10,26/. Thus, the actual composition of the gas mixtures used in the present work at the reaction temperature may be different from that of the atmospheres used previously and corresponds to lower pressures of oxygen and higher pressures of sulfur. In fact, the initial compositions of the present gas mixtures are different from those used previously /23-25/. This conclusion points out the importance of the initial composition of the gas mixtures used and of their equilibration under the actual reaction conditions. Another possible reason for the discrepancy between the present and the previous results concerning the corrosion of 310 SS in the mixture more dilute in H_2S is that in previous experiments the combination of a reduced gas flow and a large number of samples may have produced a depletion of H_2S in the gas, thus displacing its actual composition towards sulfur pressures lower than calculated for the equilibrium and, therefore, favoring the growth of oxide scales.

The structure of the scales formed by corrosion in both the present mixtures shows that nickel is only slightly corroded in this material but tends to become enriched in a surface layer in the alloy, while iron and chromium are the main scale components. In particular, iron is able to diffuse faster and becomes enriched in the outer layer of the scale. In comparison with the corrosion of the same material in H_2-H_2S mixtures under a sulfur pressure of $3.9x10^{-4}$ atm at 637°C and under a sulfur pressure of $1.4x10^{-7}$atm at 660°C /17/, corrosion in the present mixed atmospheres is slower, while the nickel content of the scales is higher. In fact, the rate constants reported by Rao and Nelson are equal to $1.7x10^{-8}$ and $2.8x10^{-8}$ $g^2cm^{-4}s^{-1}$ at 637 and 660°C, respectively /17/, while those obtained here range between 2.5 and $5x10^{-10}$ $g^2cm^{-4}s^{-1}$. This decrease in the corrosion rate is partly due to the lower temperature used in this work but also partly probably to the lower sulfur pressure, which is only slightly higher than the pressure for the Ni-Ni_3S_2 equilibrium which at 600°C amounts to $4x10^{-12}$ atm /27/. The presence of small amounts of nickel in the scales especially in the outer zone is attributed to the formation of solid solutions of nickel sulfide in the iron sulfide under activities lower than

unit, so that nickel sulfidation is permitted even under sulfur pressures smaller than for the dissociation of the lowest nickel sulfide.

So far, the corrosion of the model alloy has been studied only in coal gasification type mixtures at 550°C /26/. However, since its composition is not very different from that of alloy 800 which contains 19-23 wt % Cr and 30-35 wt % Ni, its behavior should be somewhat similar to that of this material. Studies regarding the sulfidation of alloy 800 in H_2-H_2S mixtures below 600°C done before 1978 were summarized by Perkins /28/, while the general sulfidation behavior of ternary Fe-Cr-Ni alloys was critically examined more recently by Young /18/. Apparently no detailed study of the pure sulfidation of the alloy 800 with special attention to the nature and composition of the scales has been done recently. The conclusion which may be drawn from an examination of the available data regarding the corrosion of Fe-Cr and Fe-Ni-Cr alloys is that the presence of nickel should not modify significantly the rate of corrosion of the Fe-Cr alloys as long as the concentration of chromium is sufficient to form an internal layer of chromium sulfide, which controls the overall rate of alloy sulfidation /18/. This prediction applies both when the sulfur pressure is sufficiently low to prevent the participation of nickel to sulfidation and when nickel can take part in the corrosion process by diffusing outwards to form an outer layer of iron and nickel sulfide /18/. Finally, formation of an outermost very porous layer of iron and nickel sulfide was observed during the sulfidation of Fe-Ni alloys /29,30/.

Corrosion of alloy 800 in coal gasification atmospheres has been studied many times; results available up to 1978 were collected by Perkins /28/ and those up to 1989 were critically examined by Gesmundo /6,12/. As for 310 SS, the corrosion of alloy 800 in these environments may involve the formation of oxide scales, but also of mixed oxide-sulfide or even of pure sulfide scales depending on the experimental conditions adopted. The location of the kinetic boundary was also reported for this alloy for some temperatures /20-22/ and is similar to that observed for 310 SS /6,12/.

A recent paper by Bakker et al. /26/ examined the corrosion behavior of the V-containing model alloy used in this study as well as that of two other alloys of very similar composition, one containing niobium and one free from refractory elements, in two gasification atmospheres at 550°C. One of these mixtures contained initially only CO, CO_2, H_2 and H_2S (dry gas or gas 1), while the second mixture contained also H_2O (wet gas or gas 2). The composition of gas 1 under conditions of equilibrium at 550°C corresponded to higher values of the sulfur pressure but to lower values of the oxygen pressure with respect to gas 2. The corrosion rates of the alloys in gas 1 were higher than in gas 2, but in both cases they formed mixed scales containing an outer layer of mixed iron, nickel and chromium sulfide and an inner layer containing oxides (Cr_2O_3 and $FeCr_2O_4$) and mixed sulfides /26/. The presence of vanadium was beneficial with respect to the base alloy for gas 1, but slightly detrimental for gas 2 /26/.

In the present work, the V-containing model alloy underwent a sulfidation attack in both the gas mixtures tested. In the case of the gas mixture containing 0.4 vol % H_2S, corrosion should have, in principle, involved mainly oxidation rather than sulfidation because the behavior of alloy 800 in coal gasification atmospheres is similar to that of 310 SS for which previous measurements have shown the formation of oxide scales in this environment /23-25/, (see above). Therefore, the same conclusions already given for 310 SS apply also to this material.

The main differences between the corrosion behavior of the two alloys examined here are related to the much higher concentration of nickel in the scales as well as the presence of an outermost very porous layer of iron and nickel sulfides for the model alloy. The larger content of nickel in the scales growing on the model alloy is certainly related to the much higher concentration of this element in the starting material, which produces higher values of the nickel activity in the alloy. The growth of the outer porous layer of iron and nickel sulfide is similar to that observed previously in the sulfidation of binary Fe-Ni alloys /29,30/. Even in that case, corrosion followed a parabolic rate law, but presented two different stages. The rate constant for the second stage, which corresponded to the development of the porous layer, was higher than for the initial stage /30/. The formation of whiskers of sulfide very rich in nickel was attributed to the presence of a slow stage in

the gas-solid reaction and more precisely the dissociation of H_2S at the scale surface, and to a different catalytic activity between the iron and nickel sulfide and between the sides and the tips of the whiskers of nickel sulfide /30/. It is likely that a similar situation applies also to the sulfidation of the present model alloy, but the development of the porous layer apparently starts at the beginning of the corrosion process.

Regarding the effect of the presence of vanadium on the corrosion behavior of the model alloy, a previous study showed that this is beneficial for the isothermal corrosion at 550°C in dry gases, i.e., in environments initially free from water, while it is slightly detrimental in wet atmospheres, i.e., in gases initially containing some water vapor /26/. However, in the previous work the corrosion behavior of the V-modified model alloy was compared with that of another V-free alloy having the same base composition. The significant difference in the iron and nickel content between the two alloys used here does not permit a simple comparison to be made. In general, it may be stated that the corrosion rates of the two materials examined here are quite similar, even though the model alloy corrodes in most cases slightly more slowly. However, this material has a much greater tendency to produce an outer porous layer, while the scales contain more nickel than for 310 SS. Thus, it is concluded that the long-term resistance of the model alloy is tendentially lower than that of 310 SS. However, this is more likely a consequence of the presence of a larger concentration of nickel rather than of some vanadium in the model alloy, especially in view of the tendency of the Fe-Ni alloys to form outer porous scales observed in this study. By comparing the present results with those of the previous work /26/, we can conclude that this deleterious influence is only effective under prevailingly sulfidizing conditions.

5. CONCLUSIONS

A study of the corrosion behavior of 310 stainless steel and of a model alloy based on iron and nickel with high chromium and relatively low vanadium content in coal gasification mixtures with two different H_2S contents showed that both alloys are nearly exclusively sulfidized rather than oxidized even under relatively low sulfur pressures. In both cases, the scales contain an outer layer of iron and nickel sulfide and an inner layer especially rich in chromium plus a region of internal sulfidation or sulfidation-oxidation. The alloy richer in nickel forms scales having higher nickel content and presenting a very porous outer sulfide layer rich in nickel and iron, while vanadium tends to remain in the inner region of the scales. The corrosion rates of the two materials are very similar, but the alloy richer in nickel and vanadium is probably less corrosion-resistant in the long term due to the formation of the outer porous layer. Under the present sulfidizing conditions, vanadium seems to have a negligible influence on the corrosion behavior of the model alloy, while the formation of porous scales seems to be typical of corrosion under sulfidizing conditions and to be related to the larger nickel content of this alloy with respect to 310 SS.

6. ACKNOWLEDGEMENT

L.C. Li is grateful to the European Community for a grant under which this work was done.

7. REFERENCES

1. K. Natesan, in: *High Temperature Corrosion*, R.A. Rapp, Ed., NACE, Houston (1983), p. 336.
2. R. Perkins, in: *High Temperature Corrosion*, R.A. Rapp, Ed., NACE, Houston (1983), p. 345.
3. K. Natesan, *Corrosion*, **41**, 646 (1985).
4. J. Stringer, in: *High-Temperature Oxidation and Sulfidation Processes*, J.D. Embury, Ed., Pergamon Press, New York (1990), p. 257.
5. K. Natesan, in: *Materials for Coal Gasification*, W.T. Bakker, S. Dapkunas and V. Hill, Eds., ASM International, Materials Park (1988), p. 51.
6. F. Gesmundo, in: *High Temperature Materials for Power Engineering 1990*, E. Bachelet, Ed., Kluwer Academic Pub., Dordrecht (1990), Vol. I, p. 67.
7. S. Mrowec and K. Przybylski, *High Temp. Mater. and Proc.*, **6**, 1 (1984).

8. S. Mrowec and J. Janowski, in: *Defect Chemistry of Solids,* O. Johannesen and A.G. Andersen, Eds., Elsevier, Amsterdam (1988), p. 55.
9. M.A.H. Howes, in: *Materials for Coal Gasification,* W.T. Bakker, S. Dapkunas and V. Hill, Eds., ASM International, Materials Park (1988), p. 9.
10. R.A. Perkins, in: *Corrosion Resistant Materials for Coal Conversion Systems,* D.B. Meadowcroft and M.I. Manning, Eds., Applied Sci. Pub., London (1983), p. 181.
11. D.B. Meadowcroft, *Materials Sci. and Engin.,* A 121, 669 (1989).
12. F. Gesmundo, Report to the European Community EUCO/MCS/08-1991, Bruxelles (1991).
13. D.J. Baxter and K. Natesan, *Corr. Sci.,* **26**, 153 (1986).
14. D.J. Baxter and K. Natesan, in: *Proc. 3rd Berkeley Conference on Corrosion-Erosion-Wear of Materials at Elevated Temperatures,* A.V. Levy, Ed., NACE, Houston (1987), p. 309.
15. D.J. Baxter and K. Natesan, *Oxid. Met.,* **31**, 305 (1989).
16. D.B. Rao and H.G. Nelson, in: *Properties of High Temperature Alloys,* Z.A. Foroulis and F.S. Pettit, Eds., The Electrochemical Soc., Princeton (1976), p. 464.
17. D.B. Rao and H.G. Nelson, *Oxid. Met.,* **12**, 111 (1978).
18. D.J. Young, *Rev. on High Temp. Mater.,* 4, 299 (1980).
19. A. Rahmel, M. Schorr, A. Velasco-Tellez and A. Pelton, *Oxid. Met.,* **27**, 199 (1987).
20. T.C. Tearney and K. Natesan, *J. Mater. for Energy Systems,* **1**, 16 (1980).
21. K. Natesan and M.B. Delaplane, in: *Corrosion-Erosion Behavior of Materials,* K. Natesan, Ed., Met. Soc. AIME, New York (1980), p. 1.
22. K. Natesan, in: *Corrosion-Erosion-Wear of Materials in Emerging Fossil Energy Systems,* A.V. Levy, Ed., NACE, Houston (1982), p. 100.
23. R. Santorelli, F. Bregani and J.F. Norton, *La Metall. Ital.,* **83**, 1113 (1991).
24. R. Santorelli, J.F. Norton and F. Bregani, *Proc. 11th Intern. Corrosion Congress,* AIM, Milano (1990), Vol. IV, p. 1.
25. J.F. Norton, D.J. Baxter, R. Santorelli and F. Bregani, to be published in Proc. Intern. Conf. on Advances in Corrosion and Protection, Manchester, July (1992).
26. W.T. Bakker, J.A. Bonvallet and J.H.W. deWit, to be published in Proc. Intern. Conf. on Advances in Corrosion and Protection, Manchester, July (1992).
27. R.C. Sharma and Y.A. Chang, *Met. Trans.,* **11 B**, 139 (1980).
28. R.A. Perkins, in: *Alloy 800,* W. Betteridge, Ed., North-Holland Pub. Co., Amsterdam (1978), p. 213.
29. J.P. Orchard and D.J. Young, *J. Electrochem. Soc.,* **136**, 545 (1989).
30. J.P. Orchard and D.J. Young, *Oxid. Met.,* 31, 105 (1989).